PMM U.S.S.R.,Vol.53,No.6,pp.779-786,1989
Printed in Great Britain

0021-8928/89 $10.00+0.00

NON-STATIONARY SUPERSONIC MOTION OF A COMPLEX DISCONTINUITY*

A.S. BYKOVTSEV and D.B. KRAMAROVSKII

An exact analytic solution is constructed for the non-stationary plane problem of a fracture area starting at supersonic speed on which a complex fracture process (shear with cleavage) is given. To describe the fracture process occurring at the discontinuity, a kinematic approach is used for which the magnitude and direction of the dislocation vector on the discontinuity are given on the whole fracture area as a boundary condition. Laplace and Fourier transforms are used to obtain the solution, and the Cagniard-de Hoop method is used to invert the solution. Singularities of the displacement fields are investigated in the elastic and shock waves that occur in the supersonic motion of the discontinuity, and a detailed analysis is given of the solutions obtained.

Stationary problems on the propagation of slits for a range of velocities lying between the shear wave and compressional wave velocities /1-3/ as well as problems on the supersonic cleavage of an elastic and elastic-plastic medium /4-7/ were examined in investigating fracture processes occurring at velocities exceeding the velocity of elastic wave propagation in the medium. Despite the significant number of papers devoted to the dynamics of discontinuities, the question of the displacement fields originating for a discontinuity propagating non-stationarily at a supersonic velocity has not been investigated in practice. The main purpose of this paper is to obtain and analyse wave fields for a dislocation discontinuity starting at a supersonic velocity. An analysis of wave fields for subsonic propagation velocities of dislocation discontinuities is given in /8-13/.

1. Formulation of the problem. Let a generalized dislocation discontinuity on which a constant jump of the displacement vector $[\mathbf{U}(U_x, U_y, U_z)] = \mathbf{B}(B_x, B_y, B_z) = \text{const}$ is given (the left end of the discontinuity is at rest and coincides with the z axis) start be propagate at a constant velocity v from the origin of a Cartesian system of coordinates xyz along the positive direction of the x axis in a homogeneous elastic isotropic medium at an initial time $t = 0$. We will assume that the discontinuity starts at a supersonic velocity, i.e., $v > c_p > c_s$ (c_p and c_s are the longitudinal and transverse wave velocities), while the dimension of the discontinuity along the z axis is quite large (the plane problem; the z axis is perpendicular to the plane, Fig.1). The initial conditions are zero, and the medium is at rest at infinity.

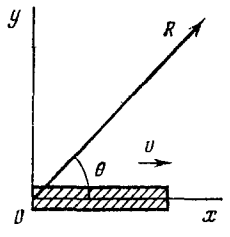

Fig.1

The generalized dislocation discontinuity can be represented in the form of the sum of shear, cleavage, and antiplane shear discontinuities. Then we have at the upper edge of the discontinuity for $y = 0$:

For the shear discontinuity

$$U_x = {}^1/_2 B_x H(x)\, H(t - xv^{-1}), \quad \sigma_{yy} = 0 \tag{1.1}$$

For the cleavage discontinuity

$$U_y = {}^1/_2 B_y H(x)\, H(t - xv^{-1}), \quad \sigma_{xy} = 0 \tag{1.2}$$

For the antiplane shear discontinuity

$$U_z = {}^1/_2 B_z H(x)\, H(t - xv^{-1}) \tag{1.3}$$

where H is the Heaviside unit function. The displacements on the lower edge of the discontinuity have the same magnitude but opposite sign.

The problem of determining the wave field being generated by a dislocation discontinuity starting at a supersonic velocity reduces to solving a system of equations for the potentials φ and ψ as well as for components U_z that have the form

$$\varphi_{,xx} + \varphi_{,yy} = c_p^{-2}\varphi^{\cdot\cdot}, \quad \psi_{,xx} + \psi_{,yy} = c_s^{-2}\psi^{\cdot\cdot}, \quad U_{z,xx} + U_{z,yy} = c_s^{-2}U_z^{\cdot\cdot} \tag{1.4}$$

(under given boundary conditions (1.1)-(1.3) and zero initial conditions), where the comma before a subscript denotes the derivative with respect to the corresponding coordinate while

*Prikl.Matem.Mekhan.,53,6,983-991,1989

the dot denotes the derivative with respect to time.

The potentials φ and ψ are connected with the components of the displacement vector by the relationships

$$U_x = \varphi_{,x} + \psi_{,y}, \quad U_y = \varphi_{,y} - \psi_{,x} \tag{1.5}$$

The components of the stress tensor are defined as follows:

$$\sigma_{ij} = \lambda U_{k,k}\delta_{ij} + \mu (U_{i,j} + U_{j,i}) \tag{1.6}$$

where δ_{ij} is the Kronecker delta and λ and μ are Lamé constants.

2. Construction of the solution. We will obtain the solution of this problem by applying Laplace and Fourier transformations

$$f_L(x, y, k) = \int_0^\infty f(x, y, t) \exp(-kt)\, dt \tag{2.1}$$

$$f_F(\xi, y, t) = \frac{1}{\sqrt{2\pi}} \int_{-\infty}^{\infty} f(x, y, t) \exp(-i\xi x)\, dx$$

and using the Cagniard-de Hoop method to invert the solution.

Applying the transformation (2.1) to (1.4) and (1.5) we obtain

$$\begin{gathered} \varphi_{LF} = C \exp(-yn_p), \quad \psi_{LF} = C_1 \exp(-yn_s) \\ U_{xLF} = i\xi C \exp(-yn_p) - C_1 n_s \exp(-yn_s) \\ U_{yLF} = -Cn_p \exp(-yn_p) - i\xi C_1 \exp(-yn_s) \\ U_{zLF} = C_2 \exp(-yn_s); \quad n_{p,s}^2 = k^2 c_{p,s}^{-2} + \xi^2 \end{gathered} \tag{2.2}$$

Applying the transformation (2.1) alternately to (1.1)-(1.3) and taking account of (2.2) we obtain systems of linear algebraic equations to determine the unknown constants C, C_1, C_2. From these systems we find:

for the shear discontinuity

$$C = A_1 B_x \cdot 2i\xi, \quad C_1 = -A_1 B_x (k^2 c_s^{-2} + 2\xi^2) n_s^{-1}$$

for the cleavage discontinuity

$$C = -A_1 B_y (k^2 c_s^{-2} + 2\xi^2) n_p^{-1}, \quad C_1 = -A_1 B_y \cdot 2i\xi$$
$$A_1 = c_s^2 [2k^3 \sqrt{2\pi}\, (kv^{-1} + i\xi)]^{-1}$$

for the antiplane shear discontinuity

$$C_2 = B_z [2\sqrt{2\pi}\, k (kv^{-1} + i\xi)]^{-1}$$

Substituting the values found for C, C_1 and C_2 into (2.2), we obtain, after making the replacement of variables, $\xi = -ikPc_p^{-1}$ and applying the inverse Fourier transformation

$$U_{jL}^{p,s} = -\frac{i}{4\pi k \beta^2} \int_{-i\infty}^{i\infty} \frac{F_j^{p,s} dP}{P + \gamma} \exp[kc_p^{-1}(Px - ym_{p,s})] \tag{2.3}$$

$$j = x, y, z, \quad m_{p,s}^2 = \beta_{p,s}^2 - P^2, \quad \gamma = c_p v^{-1}, \quad \beta_p = 1, \quad \beta_s = \beta = c_p c_s^{-1}$$

for the shear discontinuity

$$F_x^p = 2B_x P^2, \quad F_x^s = B_x (\beta^2 - 2P^2)$$
$$F_y^p = -2B_x P m_p, \quad F_y^s = B_x P (\beta^2 - 2P^2) m_s^{-1}$$

for the cleavage discontinuity

$$F_x^p = -B_y P (\beta^2 - 2P^2) m_p^{-1}, \quad F_x^s = 2B_y P m_s$$
$$F_y^p = B_y (\beta^2 - 2P^2), \quad F_y^s = 2B_y P^2$$

and for the antiplane shear discontinuity $F_z^s = B_z \beta^2$; the remaining values of $F_j^{p,s}$ equal zero.

Expression (2.3) in the time domain is inverted by the Cagniard method /14/. We define

the Cagniard contour as follows

$$t = -(Px - ym_{p,s})\, c_p^{-1}$$

We then obtain

$$P = -\tau\cos\theta \pm iT_{p,s}\sin\theta, \quad m_{p,s} = \tau\sin\theta \pm iT_{p,s}\cos\theta \tag{2.4}$$

$$T_{p,s}^2 = \tau^2 - \beta_{p,s}^2, \quad \tau = tcpR^{-1}, \quad R^2 = x^2 + y^2, \quad \operatorname{tg}\theta = y/x$$

The first of relationships (2.4) determines the branch of a hyperbola in the complex P plane for $\tau > \beta_p$, (Fig.2). Part of the contour $\Gamma_{p,s}^+$ corresponds to the plus sign in (2.4) while $\Gamma_{p,s}^-$ corresponds to the minus sign. For $\tau < \beta_{p,s}$ the Cagniard contour coincides with the axis Re P (this part of the contour is not shown in Fig.2).

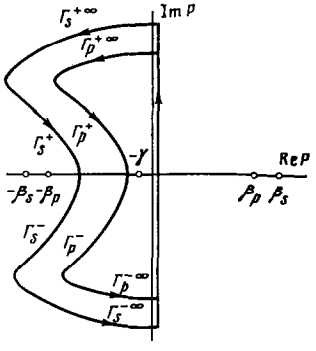

Fig.2

We pass from integration over the imaginary axis to integration over the closed contour (Fig.2). The singularities of the integrand in (2.3) are the branch points $P = \pm\beta_{p,s}$ and the pole $P = -\gamma$. The branch points lie outside the Cagniard contour. The location of the pole $P = -\gamma$ ($\gamma = c_p v^{-1}$) is determined by the magnitude of the velocity of discontinuity propagation. It follows from the first relationship of (2.4) that the pole lies outside the Cagniard contour for subsonic values of the velocity v while the pole lies within the contour for supersonic values of v for points with coordinates

$$x > \pm\, y\gamma/\sqrt{\beta_{p,s}^2 - \gamma^2} = x_{p,s}$$

Using the theorem on residues and taking into account that the integrals along Γ^∞ equal zero according to the Jordan lemma, as well as the fact that the integrand in (2.3) has an even real part and an odd imaginary part, we arrive at the relationship ($D_{jL}^{p,s}$ is the residue at the pole $P = -\gamma$)

$$U_{jL}^{p,s} = k^{-1}M_{jL}^{p,s} + D_{jL}^{p,s} \tag{2.5}$$

$$M_{jL}^{p,s} = \frac{c_p}{2\pi\beta^2 R}\operatorname{Re}\left[\int_{Rc_p^{-1}\beta_{p,s}}^{\infty} \frac{F_j^{p,s}m_{p,s}}{(P+\gamma)\,T_{p,s}}\exp(-kt)\,dt\right]$$

$$D_{jL}^{p,s} = {}^1/_2 k^{-1}\beta^{-2}F_j^{p,s}\exp\left[kc_p^{-1}(-\gamma x - ym_{p,s})\right]H(x - x_{p,s})$$

where P is replaced by $-\gamma$ in the quantities $F_j^{p,s}$ and $m_{p,s}$ in the last expression in (2.5), and this expression is itself tabulated for the Laplace transform. The expression $M_{jL}^{p,s}$ is the direct Laplace transform of the integrand in the exponential.

Taking account of the properties of the Laplace transform /15/, we obtain

$$U_j^{p,s} = \int_0^t M_j^{p,s}\,dt + D_j^{p,s} \tag{2.6}$$

$$M_j^{p,s} = \frac{c_p}{2\pi\beta^2 R}\operatorname{Re}\left[\frac{F_j^{p,s}m_{p,s}}{(P+\gamma)\,T_{p,s}}\right]H(\tau - \beta_{p,s})$$

$$D_j^{p,s} = {}^1/_2\beta^{-2}F_j^{p,s}H(t - t_{p,s})\,H(x - x_{p,s})$$

$$t_{p,s} = (x + y\sqrt{\beta_{p,s}^2\gamma^{-2} - 1})/v$$

Relationship (2.6) can be integrated analytically and we represent the final result in the following form:

$$U_z^s = AB_z\beta^2\operatorname{arc}_1^s H_s + D_z^s \tag{2.7}$$

$$U_x^p = A\{B_x[2\gamma^2\operatorname{arc}_1^p - F_p] + B_y[(1+\beta_3^2)\ln^p -$$
$$\beta_3^2\gamma\gamma_p^{-1}\operatorname{arc}_2^p + f_p]\}H_p + D_x^p, \quad U_x^s = A\{B_x[F_s - \beta_3^2\operatorname{arc}_1^s] -$$
$$B_y[\beta_3^2\ln^s + 2\gamma\gamma_s\operatorname{arc}_2^s + f_s]\}H_s + D_x^s$$
$$U_y^p = A\{B_x[(2\gamma^2 - 1)\ln^p + 2\gamma\gamma_p\operatorname{arc}_2^p + f_p] +$$
$$B_y[F_p - \beta_3^2\operatorname{arc}_1^p]\}H_p + D_y^p, \quad U_y^s = A\{B_x[\beta_3^2\gamma\gamma_s^{-1}\operatorname{arc}_2^s - 2\gamma^2\ln^s - f_s] +$$
$$B_y[2\gamma^2\operatorname{arc}_1^s - F_s]\}H_s + D_y^s$$

$$F_{p,s} = (\tau\sin 2\theta + 2\gamma\sin\theta)\,T_{p,s}, \quad f_{p,s} = (\tau\cos 2\theta + 2\gamma\cos\theta)\,T_{p,s},$$

$$\ln^{p,s} = \ln \frac{T_{p,s} + \tau}{\beta_{p,s}}, \quad \operatorname{arc}_1^{p,s} = \operatorname{arctg} \frac{T_{p,s} \sin\theta}{\gamma - \tau\cos\theta}$$

$$H_{p,s} = H(\tau - \beta_{p,s}), \quad T_{p,s} = \sqrt{\tau^2 - \beta_{p,s}^2}, \quad \tau = tc_p/R$$

$$\beta_s^2 = 2\gamma^2 - \beta^2, \quad A = 1/(2\pi\beta^2)$$

for subsonic values of v

$$\gamma_{p,s} = \sqrt{\gamma^2 - \beta_{p,s}^2}, \quad D_j^{p,s} = 0 \quad (j = x, y, z) \tag{2.8}$$

$$\operatorname{arc}_2^{p,s} = {}^1/_2 \ln \frac{(\tau\gamma_{p,s} - \gamma T_{p,s})^2 \sin^2\theta + [\beta_{p,s}^2 - (\tau\gamma - \gamma_{p,s}T_{p,s})\cos\theta]^2}{\beta_{p,s}^2[(\gamma - \tau\cos\theta)^2 + (T_{p,s}\sin\theta)^2]}$$

for supersonic values of v

$$\gamma_{p,s} = \sqrt{\beta_{p,s}^2 - \gamma^2} \tag{2.9}$$

$$D_x^p = \frac{B_x}{\beta^2}\gamma^2 H_{p1} + \frac{B_y}{2\beta^2}\frac{\beta^2 - 2\gamma^2}{\sqrt{1-\gamma^2}}\gamma H_{p1}$$

$$D_y^p = \frac{B_x}{\beta^2}\gamma\sqrt{1-\gamma^2}\,H_{p1} + \frac{B_y}{2\beta^2}(\beta^2 - 2\gamma^2)H_{p1}$$

$$D_x^s = \frac{B_x}{2\beta^2}(\beta^2 - 2\gamma^2)H_{s1} - \frac{B_y}{\beta^2}\gamma\sqrt{\beta^2 - \gamma^2}\,H_{s1}$$

$$D_y^s = -\frac{B_x}{2\beta^2}\frac{\beta^2 - 2\gamma^2}{\sqrt{\beta^2 - \gamma^2}}\gamma H_{s1} + \frac{B_y}{\beta^2}\gamma^2 H_{s1}$$

$$D_z^s = {}^1/_2 B_z H_{s1}; \quad H_{p,s1} = H(t - t_{p,s})H(x - x_{p,s})$$

$$\operatorname{arc}_2^{p,s} = \arcsin \frac{T_{p,s}\gamma_{p,s}}{\beta_{p,s}\sqrt{(\tau - \gamma\cos\theta)^2 + \gamma_{p,s}^2\sin^2\theta}}$$

*3. **Analysis of the results.*** The solutions (2.7) for subsonic values of v agree with the solutions obtained by the method of functionally invariant Smirnov-Sobolev solutions /8/. The appearance of the quantities $D_j^{p,s}$ in the solutions corresponds to supersonic propagation of the discontinuity. The part of the solution (2.7) corresponding to subsonic (supersonic) motion of the discontinuity is used for the P-waves (S-waves) for transonic motion of the discontinuity ($c_s < v < c_p$).

The domain of action of the supersonic solution is determined by the unit functions $H(t - t_{p,s})$ and $H(x - x_{p,s})$ in (2.6). This domain is bounded by the lines t_p, t_s and x_p, x_s. The lines x_p and x_s make angles $\varphi_p = \arccos\gamma$ and $\varphi_s = \arccos(\gamma/\beta)$ respectively with the x axis. Consequently, the general wave pattern will consist of circular domains representing the longitudinal and tranverse wave fronts and conelike domains bounded by the lines t_p, t_s and x_p, x_s due to supersonic motion of the discontinuity (Fig.3). The surface $t_{p,s}$ can also be considered as plane waves existing in the domain $x > x_{p,s}$ and propagating along the rays $x_{p,s}$ while the wave surfaces $\tau = \beta_{p,s}$ exist in all space.

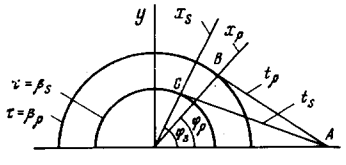

Fig.3

We will investigate the quantities $D_j^{p,s}$ defined by (2.6) in greater detail. For a shear discontinuity these quantities equal the first component of the expressions for $D_{x,y}^{p,s}$ in (2.9), for the cleavage discontinuity it is the second component, and for the antiplane shear discontinuity the quantity D_z^s is defined in (2.9). The quantities mentioned depend only on the ratio between the bulk wave velocities and the velocity of discontinuity and are independent of the time and coordinates of the observation point, which corresponds to a jump in the solution (2.7) for supersonic values of v. The domain $x > x_{p,s}$ is characterized by the fact that perturbations caused by the supersonic motion of the discontinuity arrive first at points of this part of space, and then the bulk elastic waves arrive. Only elastic waves arrive at points of the domain $x < x_{p,s}$ (Fig.3).

The direction of the jump in the displacement for a conelike "supersonic" surface (SS) in the P-waves is perpendicular to the conical wave front (the line AB, Fig.3), and in the S-waves is parallel to the conical front (the line AC, Fig.3). The direction of the displacement jump for the antiplane shear discontinuity is perpendicular to the plane of Fig.3, while the magnitude of the displacement jump depends on neither the ratio between the bulk wave velocities

nor the velocity of spread of the discontinuity.

Under practical conditions the discontinuities being propagated are usually a complex combination of shear and cleavage discontinuities. Consequently, from the viewpoint of practical applications, it is interesting to analyse the displacement fields within the cone-like "supersonic" domain as a function of the magnitudes of the cleavage and shear components of the displacement vector at the discontinuity, as well as on the velocity of spread of the discontinuity. Determining the total mangitude of the jumps D^p and D^s in P- and S-waves for the domain mentioned we obtain for a complex discontinuity $(B_x = B\cos\alpha,\ B_y = B\sin\alpha,\ B_z = 0)$

$$D^p = \gamma B\beta^{-2}(\cos\alpha + \delta_p \sin\alpha) H_{p1},\quad D^s = \gamma B\beta^{-2}(\delta_s \cos\alpha - \sin\alpha) H_{s1} \tag{3.1}$$

$$\delta_p = \frac{\beta^2 - \gamma^2}{2\gamma\sqrt{1-\gamma^2}},\quad \delta_s = \frac{\beta^2 - 2\gamma^2}{2\gamma\sqrt{\beta^2-\gamma^2}}$$

It is seen that the magnitudes of the displacement jumps in the P- and S-waves for a complex discontinuity depend very much on the angle α $(\alpha = \operatorname{arctg}(B_y/B_x))$, that the dislocation vector at the discontinuity makes with the plane of the discontinuity, (i.e., on the relationship between the shear and cleavage components of the displacement vector at the discontinuity), as well as on the velocity of spread of the discontinuity

Let us examine the following two ranges of variation of this angle $0 \leqslant \alpha \leqslant \pi/2$ and $\pi/2 < \alpha < \pi$ in greater detail.

For $0 \leqslant \alpha \leqslant \pi/2$ the direction of the shear component of the displacement vector at the upper edge of the discontinuity coincides with the direction of spread of the moving edge of the discontinuity. In this case the jumps in the displacement behind the SS in the P-waves are directed to one side for pure shear and pure cleavage discontinuities. Consequently, the maximum amplitude of the displacements in the P-wave will reach a value of

$$D^p_{\max} = {}^1/_2 B\beta^{-2}\left[\frac{\beta^4 - 4\gamma^2\beta^2 + 4\gamma^3}{1-\gamma^2}\right]^{1/2} \tag{3.2}$$

for a complex discontinuity for $0 \leqslant \alpha \leqslant \pi/2$ and $\alpha = \alpha^p_{\max} = \operatorname{arctg}\delta_p$.

The displacement jumps for the SS in the S-waves are parallel to the conical front and are directed for $0 \leqslant \alpha \leqslant \pi/2$ to different sides for the pure shear and pure cleavage discontinuities (from C to A and from A to C, respectively, in Fig.3). Consequently, for $\alpha = \alpha_0^s = \operatorname{arctg}\delta_s$ we obtain $D_0^s = 0$, i.e., despite the supersonic motion of the discontinuity, for $\alpha = \alpha_0^s$ there will be no S-wave SS and S-wave radiation will be analogous to that occuring for subsonic motion of the discontinuity.

For $\pi/2 < \alpha \leqslant \pi$ the direction of the shear component of the displacement vector at the discontinuity is opposite to the direction of spread of the moving edge of the discontinuity. In this case the displacement jumps behind the SS front in P-waves are directed to different sides for pure shear and pure cleavage discontinuities and we obtain $D_0^p = 0$ for $\alpha = \alpha_0^p = \pi/2 + \alpha^p_{\max}$ i.e., despite the supersonic motion of the discontinuity, for $\alpha = \alpha_0^p$ there will be no P-wave SS and the wave pattern of P-wave radiation will be analogous to that occurring for subsonic motion of the discontinuity.

For $\pi/2 < \alpha \leqslant \pi$ the displacement waves for S-wave SS are directed to one side for pure cleavage and pure shear discontinuities. Consequently, the maximum value of the displacement in S-waves for a complex discontinuity for $\pi/2 < \alpha \leqslant \pi$ will reach a value of

$$D^s_{\max} = {}^1/_2 B\beta/\sqrt{\beta^2-\gamma^2} \tag{3.3}$$

for $\alpha = \alpha^s_{\max} = \pi/2 + \alpha_0^s$.

Graphs of the functions D^p and D^s, respectively, are presented in Figs.4a and b in a polar system of coordinates as a function of the angle variations $\alpha\ (0 \leqslant \alpha \leqslant \pi)$ for different values of the velocity of spread of the discontinuity (curves *1, 2, 3* correspond to the values $\gamma = 0.2,\ 0.83,\ 0.95$ for $\beta = 1.9$ (chalk) and $B = 1$. The solid lines correspond to positive values of $D^{p,s}$, and the dashed lines correspond to negative values). Values of the function D^p reach maxima $D^p_{\max} = 0.5,\ 0.61,\ 0.85$ for $\alpha^p_{\max} = 80,\ 60,\ 67°$ (for curves *1, 2, 3*, respectively). The absolute values of the function D^s reach the maxima $D^s_{\max} = 0.5,\ 0.53,\ 0.58$ for $\alpha^s_{\max} = 165,\ 127,\ 113°$ (the directions in which the functions $D^{p,s}$ reach the maxima and vanish are denoted by dashed sections in Figs.4a and b).

The dependences of the values of the angles α on the velocity of spread of the discontinuity for which a maximum is reached (the solid lines) and there are no SS (the dashed lines) in the P-wave (Fig.5a) and the S-wave (Fig.5b) are presented in Fig.5 (curves *1, 2, 3* correspond to values of β of 1.7 (granite), 1.9 (chalk), and 2.44 (clay shale)). For P-waves

these curves have a minimum for $\gamma^* = \beta\,[2\,(\beta^2 - 1)]^{-1/2}$ where $\alpha_1^* = \operatorname{arctg}(\beta\sqrt{\beta^2 - 2})$ and $\alpha_2^* = \pi/2 + \alpha_1^*$.

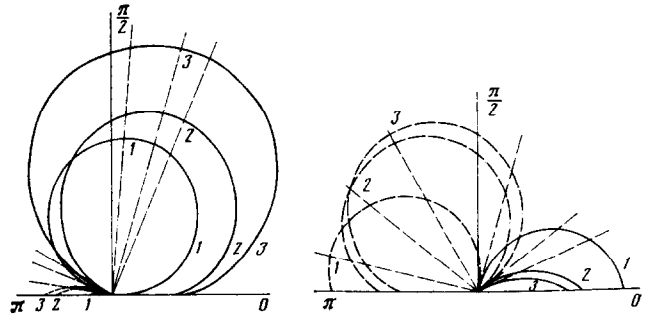

a Fig.4 b

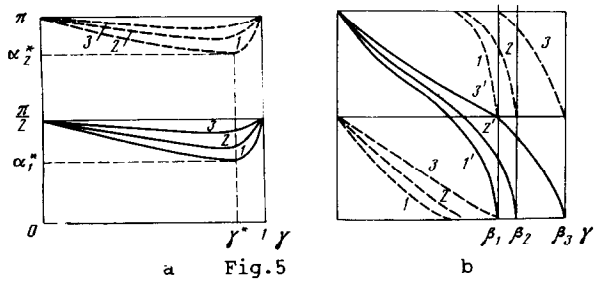

a Fig.5 b

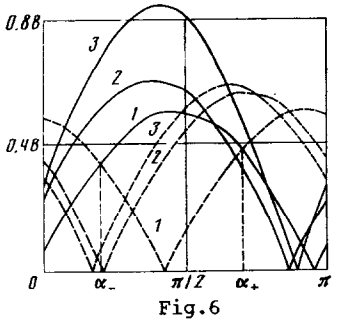

Fig.6

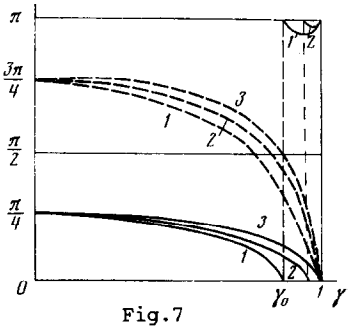

Fig.7

Analogous curves for the S-waves (Fig.5b) have no extremum point and the values of the angles for which the maximum is achieved vary montonically from π to zero as γ changes from zero to β. Values of the angles α^s_0 for which there is no displacement jump in the S-waves vary from $\pi/2$ for $\gamma = 0$ to zero for $\gamma = \beta/\sqrt{2}$ and from π to $\pi/2$ as the change $\beta/\sqrt{2} < \gamma < \beta$.

We know from an analysis of the radiation patterns of seismic radiation in P- and S-waves /8, 9, 11-13/ for a discontinuity propagating at the velocity $v < c_s < c_p$ that, as a rule, the absolute magnitude of the displacement amplitude in S-waves exceeds by an order the magnitude of the displacement amplitude in P-waves. The orders of magnitude of displacements behind the SS front in P- and S-waves are identical for supersonic motion of a discontinuity with velocity $v > c_p > c_s$.

Absolute values of the displacement amplitudes D^p (the solid lines) and D^s (the dashes) are shown in Fig.6 for different values of γ (curves *1*, *2*, *3*, correspond to the values $\gamma = 0.2$; 0.83, 0.95 for $\beta = 1.9$). It follows from an analysis of Fig.6 as well as of (3.1) that the absolute value of the displacement jump in P-waves will be greater than the displacement jump in S-waves for $\alpha > \alpha_-$ and $\alpha < \alpha_+$ where

$$\alpha_\pm = \operatorname{arctg}\,[(\beta\delta_s \pm 1)/(\beta \mp \delta_p)]$$

and for $\alpha < \alpha_-$ and $\alpha > \alpha_+$ the absolute value of the displacement jump in S-waves is greater than the magnitude of the jump in P-waves.

The dependences of the change in the angles α_- and α_+ on the velocity of spread of the

discontinuity ($\gamma = c_p/v$) are shown in Fig.7 for $\beta = 1.7, 1.9, 2.44$. The parameter α_+ varies between $3\pi/4$ and zero as γ changes between zero and one. The magnitude of the angle α_- for materials with the value $\beta > 1.926$ changes between $\pi/4$ and zero for $0 \leqslant \gamma \leqslant 1$ and for materials with the value $\beta < 1.926$ between $\pi/4$ and zero for $0 \leqslant \gamma \leqslant [1/2\beta^2(1-(\beta^2+1)^{-1/2})]^{1/2} = \gamma_0$.

A jump by π occurs in the function α_- for $\gamma = \gamma_0$ (Fig.7).

It follows from (3.2) and (3.3) that as $v \to \infty$ $(\gamma \to 0)$ the maximum value of the displacement jump $D^p_{\max} = B/2$ will be reached behind the SS front in the P-wave for a pure cleavage discontinuity, i.e., for $\alpha = \pi/2$. In the S-wave the maximum magnitude of the displacement jump $D^s_{\max} = B/2$ will occur for a pure shear discontinuity, i.e., for $\alpha = 0$, $\alpha = \pi$, $v \to \infty$. As $\gamma \to 1$ $(v \to c_p)$ and $\gamma \to \beta$ $(v \to c_s)$ the quantities $D^p_{\max}$ and $D^s_{\max}$, respectively, tend to infinity, but the domains in which they take very large values shrink to a point, since the angles $\varphi_p = \arccos\gamma$ and $\varphi_s = \arccos(\gamma/\beta)$ (Fig.3) become infinitesimal.

It should be noted that the solutions (2.7)-(2.9) constructed are obtained under the condition that the vector $\mathbf{B} = \text{const}$. Consequently, they are a certain mathematical idealization of actual physical processes. For a more practical simulation of the physical processes on the surface of discontinuity, the dislocation vector should be given in the form of a certain function which depends on the coordinates and time. On the basis of the linearity of the fundamental equations the solution of the problem with an arbitrary dislocation vector on the discontinuity can be obtained by applying the convolution operation to the solutions (2.7)-(2.9) constructed. Consequently, by considering (2.7)-(2.9) as solutions obtained in generalized functions, they can be utilized effectively to construct the solutions of a number of more-general problems.

The question of whether or not the deductions made on the basis of the solution obtained are conserved after applying the convolution operation is of interest. In our opinion, qualitative effects associated with the behaviour of the radiation pattern of seismic radiation on a conelike surface caused by the supersonic motion of a discontinuity are conserved.

The solution of the problem when a constant velocity jump is given on the discontinuity can be considered as an example. Then the surface of discontinuity will have the shape of a thin wedge and the dislocation vector $\mathbf{B}_1$ on the discontinuity will depend linearly on the time t. In this case the velocity field will be given by (2.7)-(2.9) and the solutions (2.7)-(2.9) should be integrated over the time t to obtain the total displacement field. Therefore, the displacement field in the problem of the supersonic motion of a discontinuity with a constant velocity jump can be represented in the form

$$U_j^{p,s} = \int_{t_{0p,s}}^{t} U_{1j}^{p,s}(x, y, \tau)\, d\tau + D_j^{p,s}(t - t_{p,s}) \tag{3.4}$$

where $U_{1j}^{p,s}$ are functions from the relationships (2.7) that stand for the unit functions $H_{p,s}$; $D_j^{p,s}$ are determined in (2.7) and (2.9), $t_{0p,s}$ are the arrival times of the bulk P- and S-waves at the observation point, and $t_{p,s}$ is the arrival time of the "supersonic" waves at the observation point.

Analysis of the results obtained indicates that the solution in the "supersonic" domain is already determined by smooth functions without discontinuities and which depend linearly on the time. The nature of the behaviour of this solution is the same as the solutions (2.7)-(2.9), i.e., the deduction made on the basis of an analysis of the results in (2.7)-(2.9) are conserved in general. The distinction will be that for Figs.4 and 6 it is necessary to indicate at precisely what times these graphs have been constructed.

Thus, if graphs analogous to those presented in Fig.4 are constructed by means of the solution (3.4), then their form will be identical with the graphs in Fig.4 if for P-waves they were constructed at that time t_1 such that $t_1 - t_p = 1$, and for S-waves at a time t_2 such that $t_2 - t_s = 1$. If graphs analogous to those presented in Fig.6 are constructed from the solution (3.4), then their form will be identical with the graphs of Fig.6, if they are constructed at the time t_3 for P-waves and the time t_4 for S-waves such that $t_3 - t_p = t_4 - t_s$.

REFERENCES

1. SLEPYAN L.I. and FISHKOV A.L., The problem of the propagation of a discontinuity at an intersonic velocity, Dokl. Akad. Nauk SSSR, 261, 6, 1981.
2. SIMONOV I.V., On the behaviour of the solutions of dynamic problems in the neighbourhood of the edge of a slit moving at transonic velocity in an elastic medium, Izv. Akad. Nauk SSSR, Mekhan. Tverd. Tela, 2, 1983.
3. SIMONOV I.V., Transonic flow around a thin solid by an elastic medium, PMM, 48, 1, 1984.

4. PAVLENKO A.L. and APIKYAN ZH.G., Supersonic flow around a stiff wedge by a linearly elastic medium, Izv. Akad. Nauk UzbekSSR, Ser. Tekh. Nauk, 2, 1969.
5. BORZYKH A.A. and CHEREPANOV G.P., On the theory of the fracture of solids subjected to powerful electron beam pulses, PMM, 44, 6, 1980.
6. BORZYKH A.A., A spatial selfsimilar problem on the supersonic cleavage of an elastic body, PMM, 45, 2, 1981.
7. BYKOVYSEV G.I., KOLOKOL'CHIKOV A.V. and SYRGUNOV P.N., Selfsimilar solutions of the equations of the dynamics of an ideal elastic plastic body under Tresca plasticity conditions, Prikl. Mekhan. Tekh. Fiz., 6, 1984.
8. BYKOVTSEV A.S., Propagation of complex discontinuities with piecewise-constant and variable velocities along curvilinear and branching trajectories, PMM, 50, 5, 1986.
9. BYKOVTSEV A.S., Modelling of fracture processes occurring in the focal zone of a tectonic earthquake, Proc. Intern. Conf. on Computational Mechanics, 1, Pt.3. Springer-Verlag, Berlin, 1986.
10. MADARIAGA R., The dynamic field of Haskell's rectangular dislocation fault model, Bull. Seismol, Soc. Amer., 68, 4, 1978.
11. BYKOVTSEV A.S., On wave fields produced by propagating dislocation discontinuities, Experimental Seismology in Uzbekistan, Fan, Tashkent, 1983.
12. BYKOVTSEV A.S. and KRAMAROVSKY D.B., The displacement field produced by the propagating rectangular rupture plane: The exact three-dimensional solution, Proc. Intern. Conf. on Computational Mech., 2, 6, Springer-Verlag, Berlin, 1986.
13. BYKOVTSEV A.S. and KRAMAROVSKII D.B., On the propgation of a complex fracture area, Exact three-dimensional solution, PMM, 51, 1, 1987.
14. CAGNIARD L., Reflection and Refraction of Progressive Seismic Waves, McGraw-Hill, New York, 1962.
15. ABRAMOWITZ M. and STIGAN I.M., Eds. Handbook on Special Functions with Formulas, Graphs and Mathematical Tables, Nauka, Moscow, 1979.

Translated M.D.F.

PMM U.S.S.R., Vol.53, No.6, pp.786-790, 1989
Printed in Great Britain

0021-8928/89 $10.00+0.00

MOMENT THEORY OF ELECTROMAGNETIC EFFECTS IN ANISOTROPIC SOLIDS*

I.G. TEREGULOV

A moment (polar) theory of deformable solids is constructed for anisotropic media such as polarizable piezoelectric ceramics. The linear theory is considered in detail and an explanation of the non-linear change in the electric field inside a polarized piezoelectric material (the Mead effect) is given. The classical theory of electromagnetic effects in solids does not enable certain observed effects to be described (for example, the Mead effect /1/). Attempts to eliminate this drawback of classical theory /2, 3/ rest on the introduction of the polarization gradient into the enthalpy as a parameter of the process. Models of complex media which takes into account the internal mechanical and electromagnetic moments have been constructed in electrodynamics (for example /4, 5/) when electromagnetic fields interact with the medium. Below, a solution of the problem is given and an example of a natural description of the Mead effect is presented.

Suppose $x^i (i = 1, 2, 3)$ is a Lagrange system of coordinates frozen into a medium which occupies a volume V with a boundary S. The vector $\mathbf{r}(x^i, t)$, defines the position of a point of this medium with respect to a fixed inertial system y^i, where t is the time. The vector $\mathbf{r}^* = \mathbf{r} + \mathbf{u}(x^i, t)$ defines the position of material points of the medium after strain, where $\mathbf{u}$ is the displacement vector. Further constructions which are carried out have the purpose of

*Prikl. Matem. Mekhan., 53, 6, 992-997, 1989